Proceedings

The 7th International Congress of Serbian Society of Mechanics

Sremski Karlovci, June 24-26, 2019

Edited by:

Mihailo Lazarević
Srboljub Simić
Damir Madjarević
Ivana Atanasovska
Andjelka Hedrih
Bojan Jeremić

The 7th International Congress of Serbian Society of Mechanics

Editors:
Mihailo P.Lazarević
Srboljub Simić
Damir Madjarević
Ivana Atanasovska
Anđelka Hedrih
Bojan Jeremić

Circulation
140 copies

Published by
Serbian Society of Mechanics,Belgrade,2019

Printed by
Planeta Print, Belgrade, 2019

CIP - Каталогизација у публикацији - Народна библиотека Србије, Београд

531/534(082)(0.034.2)

SRPSKO društvo za mehaniku. Međunarodni kongres (9 ; 2019 ; Sremski Karlovci)
Proceedings [Elektronski izvor] / The 7th International Congress of Serbian Society of Mechanics, Sremski Karlovci, June 24-26, 2019 ; edited by Mihailo Lazarević ... [et al.]. - Belgrade : Serbian Society of Mechanics, 2019 (Belgrade : Planeta Print). - 1 USB fleš memorija ; 9 x 5 cm (u obliku kartice)

Sistemski zahtevi: Nisu navedeni. - Nasl. sa naslovne strane dokumenta. - Tiraž 140. - Bibliografija uz svaki rad.

ISBN 978-86-909973-7-4

a) Механика - Зборници

COBISS.SR-ID 277232652

THREE-DIMENSIONAL STRESS ANALYSIS OF LAMINATED COMPOSITE PLATES USING FLWT-BASED FINITE ELEMENTS

Emilija V. Damnjanović[1], Miroslav S. Marjanović[2]

Faculty of Civil Engineering, University of Belgrade,
Bulevar kralja Aleksandra 73, 11000 Belgrade, Serbia
[1] e-mail: edamjanovic@grf.bg.ac.rs
[2] e-mail: mmarjanovic@grf.bg.ac.rs

Abstract

The paper deals with the 3-D stress analysis of laminated composite plates using a layerwise displacement model of Reddy, that assumes piece-wise linear variation of all displacement components and the quadratic variation of interlaminar stresses within each layer of the plate. Based on the assumed displacement field, kinematic relations, 3-D constitutive equations of both lamina and laminate and governing equations of motion have been derived. Starting from the strong formulation of the full layerwise theory (FLWT), family of layered finite elements has been developed and implemented in original object-oriented MATLAB code. GiD software is used for the pre- and post-processing.

The parametric effects of plate side-to-thickness ratio, mesh refinement in- and out-of-plane and applied element type on total deflection and stress distribution in the considered laminate are shown. The accuracy of the present model is verified against the existing data from the literature and the commercial software. The possibilities for the further improvement and applications of the model are briefly presented.

Key words: full layerwise theory, 3-D stress state, bending, laminate, composite, plate

1. Introduction

Laminar composites play a significant role in various engineering disciplines, motivating the authors to develop robust and simple computational models of laminated composite beams, plates and shells. However, many unique phenomena arising from the heterogeneous constitution of laminated composite plates (LCPs) leaded the investigators to derive complex and accurate computational models. The deformation of LCPs is characterized by the coupling between bending, extension, and shear, while at the ply level laminated composites exhibit transverse stress concentrations near material and geometric discontinuities, resulting in different forms of damage, i.e. delamination or matrix cracking.

The global behavior of LCPs (deflections, critical buckling loads, fundamental vibration frequencies and mode shapes) may be accurately predicted using equivalent-single-layer (ESL) theories [1-3], especially for very thin laminates. However, if a highly accurate assessment of the stress-deformation state is needed (for example, in localized regions where damage initiation is

likely, or in the case of thick structural component), refined theories are recommended. In addition, the assessment of localized regions for potential damage initiation begins with the accurate determination of the 3-D state of stress/strain at the ply level. The extensive review of refined laminate theories can be found in [4-6], among others.

The application of partial layerwise laminate theories has been authors' focus in development of global response of previously damaged laminates [7-9], starting from the previous research of Ćetković and Vuksanović [10]. The displacement-based partial layerwise laminate theories neglect the transverse normal stress/strain (due to the fact that deflection is constant through the thickness). However, the incorporation of the transverse normal stress σ_{zz} is important in modeling the localized effects such as holes, cut-outs or delamination fronts. Note that σ_z is significant and usually dominant in these regions. It is also important in the prediction of damage initiation.

The use of FLWT is justified due to another important fact: in all ESL theories based on the assumed displacement fields (the displacements are assumed to be continuous functions of thickness coordinate), all stresses are discontinuous at layer interfaces. More important, the interlaminar stresses τ_{xz}, τ_{yz} and σ_z are discontinuous, which does not satisfy the continuity conditions between the stress fields of the adjacent layers. This error is especially dangerous for thick laminates. In contrast to the ESL theories, the layerwise theories allow for the possibility of continuous transverse stresses at layer interfaces. Moreover, they provide a much more correct representation of cross-sectional warping.

In the paper, the full layerwise theory of Reddy [11] (FLWT) served as a basis for the development of a family of layered finite elements, accounting for the layerwise expansion of all three displacement components. Original procedure for post-processing of stresses is presented. The computational model is implemented using original object-oriented MATLAB [12] code, while the graphical user interface for pre- and post-processing is developed using GiD [13]. The presented approach is validated against the 3-D (solid) models of LCPs in ABAQUS [14], as well as using the available data from the literature.

2. Development of the strong formulation of the FLWT

In the paper, we consider laminated composite plates made of n orthotropic layers. The plate thickness is denoted as h (see Figure 1), while the thickness of the k^{th} lamina is denoted as h_k. The plate is supported along the portion Γ_u of the boundary Γ and loaded with loadings $q_t(x,y)$ and $q_b(x,y)$ acting perpendicular to either top or the bottom surface of the plate (S_t or S_b).

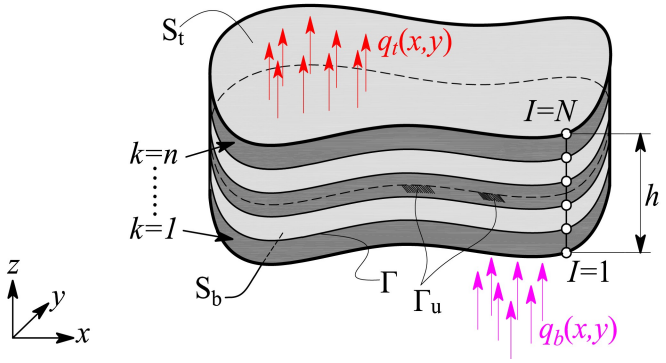

Fig. 1. Laminated composite plate with n material layers and N numerical interfaces

Piece-wise linear variation of all three displacement components is imposed, leading to the 3-D stress description of all material layers. The displacement field (u, v, w) of an arbitrary point (x,y,z) of the laminate is given as:

$$u(x,y,z)=\sum_{I=1}^{N}U^{I}(x,y)\Phi^{I}(z),\qquad v(x,y,z)=\sum_{I=1}^{N}V^{I}(x,y)\Phi^{I}(z),$$
$$w(x,y,z)=\sum_{I=1}^{N}W^{I}(x,y)\Phi^{I}(z) \tag{1}$$

In Eq. (1), $U^I(x,y)$, $V^I(x,y)$ and $W^I(x,y)$ are the displacement components in the I^{th} numerical layer of the laminate in directions x, y and z, respectively, N is the number of interfaces between the layers including S_t and S_b. Note that the number of subdivisions (I=1,2,…N) through the thickness can be greater than or equal to the number of material layers through the thickness (n).

For the sake of simplicity, $\Phi^I(z)$ are selected to be linear layerwise continuous functions of the z-coordinate:

$$\Phi^{1}(z)=1-\frac{\overline{z}}{h_1},\quad 0\le\overline{z}\le h_1,\qquad \Phi^{N}(z)=\frac{\overline{z}}{h_N},\quad 0\le\overline{z}\le h_N$$
$$\Phi^{I}(z)=\begin{cases}\dfrac{\overline{z}}{h_{I-1}}, & 0\le\overline{z}\le h_{I-1}\\ 1-\dfrac{\overline{z}}{h_I}, & 0\le\overline{z}\le h_I\end{cases},\quad I=2,3,...,N-1 \tag{2}$$

The linear strain field associated with the previously shown displacement field can be found in [11]. It serves as the basis for the derivation of 3N governing differential equations which define the strong form of the FLWT. To reduce the 3-D model to the 2-D one (plate model), the z-coordinate is eliminated by the explicit integration of stress components multiplied with the corresponding functions $\Phi^I(z)$, introducing the stress resultants which can be found in [11].

The stresses in the k^{th} layer may be computed from the lamina 3-D constitutive equations:

$$\begin{Bmatrix}\sigma_x\\ \sigma_y\\ \sigma_z\\ \tau_{yz}\\ \tau_{xz}\\ \tau_{xy}\end{Bmatrix}^{(k)}=\begin{bmatrix}\overline{C}_{11} & \overline{C}_{12} & \overline{C}_{13} & 0 & 0 & \overline{C}_{16}\\ \overline{C}_{21} & \overline{C}_{22} & \overline{C}_{23} & 0 & 0 & \overline{C}_{26}\\ \overline{C}_{31} & \overline{C}_{32} & \overline{C}_{33} & 0 & 0 & \overline{C}_{36}\\ 0 & 0 & 0 & \overline{C}_{44} & \overline{C}_{45} & 0\\ 0 & 0 & 0 & \overline{C}_{45} & \overline{C}_{55} & 0\\ \overline{C}_{16} & \overline{C}_{26} & \overline{C}_{36} & 0 & 0 & \overline{C}_{66}\end{bmatrix}^{(k)}\begin{Bmatrix}\varepsilon_x\\ \varepsilon_y\\ \varepsilon_z\\ \gamma_{yz}\\ \gamma_{xz}\\ \gamma_{xy}\end{Bmatrix}^{(k)} \tag{3}$$

where $\overline{C}_{ij}$ are the transformed elastic coefficients in the (x,y,z) coordinates, which are related to the elastic coefficients in the material (1,2,3) coordinates, C_{ij} through the transformation matrix $\mathbf{T}^{(k)}$ for the k^{th} layer. Matrices $\mathbf{C}^{(k)}$ and $\mathbf{T}^{(k)}$ can be found in [11]. The constitutive relations of the laminate can be derived in a usual manner by integrating the lamina constitutive equations through the thickness of the plate.

The system of 3N Euler-Lagrange governing equations of motion for the FLWT are derived using the principle of virtual displacements, by satisfying the equilibrium of the virtual strain energy δU and the work done by the applied forces δV (note that virtual kinetic energy δK = 0 for the static problems):

$$\frac{\partial N_{xx}^{I}}{\partial x}+\frac{\partial N_{xy}^{I}}{\partial y}-Q_x^I=0,\quad \frac{\partial N_{xy}^{I}}{\partial x}+\frac{\partial N_{yy}^{I}}{\partial y}-Q_y^I=0,\quad \frac{\partial Q_x^{I}}{\partial x}+\frac{\partial Q_y^{I}}{\partial y}-\tilde{Q}_z^I+q_b\delta_{I1}+q_t\delta_{IN}=0 \tag{4}$$

where $N_{xx}^I, N_{xy}^I, N_{yy}^I, Q_x^I, Q_y^I, \tilde{Q}_z^I$ are stress resultants defined in [11], while δ_{I1} and δ_{IN} are

displacement vectors at the S_b and S_t, respectively. The primary variables of the problem are displacement components U^I, V^I and W^I.

3. Layered FLWT-based Finite Element

Based on the FLWT, the displacement finite element model (weak form) is derived by substituting an assumed interpolation of the displacement field (1) into the equations of motion (4) of the FLWT. The layered finite elements require only C^0 continuity of generalized displacements along element boundaries, because only translational displacement components are adopted as the nodal degrees of freedom. It is important to highlight that the out of plane coordinate has been eliminated in the calculation after the explicit integration of the displacement field in out-of-plane direction. This allows the formulation of the family of the 2-D layered (plate) finite elements, allowing for the 2-D type data structure similar to the FE models of the ESL theories, which provide the following advantages against the conventional 3-D models:

- the volume of input data is reduced,
- the out of plane interpolation can be refined independently of the in-plane one, without the need to reconstruct the 3-D mesh,
- Model reduction to the 2-D one results in the computational savings in the numerical integration while constructing the element stiffness matrix. The savings are increased by increasing the number of elements and number of interfaces through the plate thickness.

All displacement components are interpolated using the same level of interpolation:

$$U^I(x,y)=\sum_{j=1}^{m}U_j^I\psi_j(x,y),\qquad V^I(x,y)=\sum_{j=1}^{m}V_j^I\psi_j(x,y),\qquad W^I(x,y)=\sum_{j=1}^{m}W_j^I\psi_j(x,y) \tag{5}$$

In (5), m is the number of nodes per 2-D element, U_j^I, V_j^I, W_j^I are the nodal values of displacements U^I, V^I and W^I, respectively, in the j^{th} node of the 2-D element representing the behaviour of the laminated composite plate in the I^{th} numerical interface. Finally, $\psi_j(x,y)$ are the 2-D Lagrangian interpolation polynomials associated with the j^{th} element node. The strain field is interpolated in the usual manner, by incorporating (5) in the kinematic relations of the FLWT. The matrix form of the finite element model is obtained as:

$$\left[K^{IJ}\right]\left\{\Delta^I\right\}=\left\{F^I\right\} \tag{6}$$

In Eq. (6), $[K^{IJ}]$ is the element stiffness matrix, $\{\Delta^I\}$ is the element displacement vector and $\{F^J\}$ is the element force vector, I=1,…,N and J=1,…,N. $[K^{IJ}]$ is obtained using 2-D Gauss-Legendre quadrature for quadrilateral domains.

In the paper, linear (Q4) and quadratic serendipity (Q8) layered quadrilateral elements have been considered. The reason is their easy connecting with the 3-node (T3) and 6-node (T6) triangular layered finite elements, which are also being developed by authors in order to represent complex plate geometries. To avoid shear locking, reduced integration is used (2×2 points for Q8 and 1×1 point for Q4 element). After the derivation of the characteristic element matrices, the assembly procedure is done in a usual manner. After the assembly procedure of the characteristic element matrices and vectors, the mathematical model on the structural level is obtained as:

$$\mathbf{Kd}=\mathbf{f} \tag{7}$$

where **K**, **d** and **f** are system stiffness matrix and system displacement and force vectors, respectively.

4. Post-Computation of Stresses

The assumed piecewise linear interpolation of displacement field through the laminate thickness provide discontinuous stresses across the interface between adjacent layers. Once the nodal displacements are obtained, the stresses can be computed from the constitutive relations:

$$\begin{Bmatrix}\sigma_x\\ \sigma_y\\ \sigma_z\\ \tau_{xy}\end{Bmatrix}_b^k = \begin{bmatrix}\bar{C}_{11} & \bar{C}_{12} & \bar{C}_{16}\\ \bar{C}_{21} & \bar{C}_{22} & \bar{C}_{26}\\ \bar{C}_{31} & \bar{C}_{32} & \bar{C}_{36}\\ \bar{C}_{61} & \bar{C}_{62} & \bar{C}_{66}\end{bmatrix}^k \sum_{j=1}^{m}\begin{bmatrix}\psi_{j,x} & 0\\ 0 & \psi_{j,y}\\ \psi_{j,y} & \psi_{j,x}\end{bmatrix}\begin{Bmatrix}U\\ V\end{Bmatrix}_j^I + \begin{Bmatrix}\bar{C}_{13}\\ \bar{C}_{23}\\ \bar{C}_{33}\\ \bar{C}_{63}\end{Bmatrix}\sum_{j=1}^{m}\psi_j\left(W_j^{I+1}-W_j^I\right)\frac{1}{h_k} \tag{7a}$$

$$\begin{Bmatrix}\sigma_x\\ \sigma_y\\ \sigma_z\\ \tau_{xy}\end{Bmatrix}_t^k = \begin{bmatrix}\bar{C}_{11} & \bar{C}_{12} & \bar{C}_{16}\\ \bar{C}_{21} & \bar{C}_{22} & \bar{C}_{26}\\ \bar{C}_{31} & \bar{C}_{32} & \bar{C}_{36}\\ \bar{C}_{61} & \bar{C}_{62} & \bar{C}_{66}\end{bmatrix}^k \sum_{j=1}^{m}\begin{bmatrix}\psi_{j,x} & 0\\ 0 & \psi_{j,y}\\ \psi_{j,y} & \psi_{j,x}\end{bmatrix}\begin{Bmatrix}U\\ V\end{Bmatrix}_j^{I+1} + \begin{Bmatrix}\bar{C}_{13}\\ \bar{C}_{23}\\ \bar{C}_{33}\\ \bar{C}_{63}\end{Bmatrix}\sum_{j=1}^{m}\psi_j\left(W_j^{I+1}-W_j^I\right)\frac{1}{h_k} \tag{7b}$$

$$\begin{aligned}\begin{Bmatrix}\tau_{yz}\\ \tau_{xz}\end{Bmatrix}_b^k &= \begin{bmatrix}\bar{C}_{44} & \bar{C}_{45}\\ \bar{C}_{54} & \bar{C}_{55}\end{bmatrix}^k \sum_{j=1}^{m}\begin{Bmatrix}\psi_{j,x}\\ \psi_{j,y}\end{Bmatrix}W_j^I + \begin{bmatrix}\bar{C}_{44} & \bar{C}_{45}\\ \bar{C}_{54} & \bar{C}_{55}\end{bmatrix}^I \sum_{j=1}^{m}\begin{bmatrix}\psi_j & 0\\ 0 & \psi_j\end{bmatrix}\left(\begin{Bmatrix}U\\ V\end{Bmatrix}_j^{I+1} - \begin{Bmatrix}U\\ V\end{Bmatrix}_j^I\right)\frac{1}{h_k}\\ \begin{Bmatrix}\tau_{yz}\\ \tau_{xz}\end{Bmatrix}_t^k &= \begin{bmatrix}\bar{C}_{44} & \bar{C}_{45}\\ \bar{C}_{54} & \bar{C}_{55}\end{bmatrix}^k \sum_{j=1}^{m}\begin{Bmatrix}\psi_{j,x}\\ \psi_{j,y}\end{Bmatrix}W_j^{I+1} + \begin{bmatrix}\bar{C}_{44} & \bar{C}_{45}\\ \bar{C}_{54} & \bar{C}_{55}\end{bmatrix}^I \sum_{j=1}^{m}\begin{bmatrix}\psi_j & 0\\ 0 & \psi_j\end{bmatrix}\left(\begin{Bmatrix}U\\ V\end{Bmatrix}_j^{I+1} - \begin{Bmatrix}U\\ V\end{Bmatrix}_j^I\right)\frac{1}{h_k}\end{aligned} \tag{8}$$

where $\psi_{j,x}$, $\psi_{j,x}$ denotes differentiation of ψ_j by x, y, respectively, *b=bottom* and *t=top*.

Since the interlaminar stresses calculated in this way does not satisfy continuous distribution through the laminate thickness, they can be computed by assuming the quadratic distribution within each layer for every stress component, separately:

$$\bar{\boldsymbol{\tau}}^k = \left\{\tau_{xz}^k \quad \tau_{yz}^k \quad \sigma_z^k\right\} = a_s^k\bar{z}^2 + b_s^k\bar{z} + c_s^k, \qquad k = 1,2,...,N, \qquad s = xz,\ yz \text{ or } z. \tag{9}$$

This require *3N* equations for each of interlaminar stresses, where *N* is the number of layers. These equations can be obtained from the following conditions:

1. satisfying the traction boundary conditions at S_b and S_t (2 equations)

$$\bar{\tau}^1\left(\bar{z}=0\right) = q_b, \qquad \bar{\tau}^N\left(\bar{z}=h_N\right) = q_t \tag{10a}$$

2. providing the continuity of interlaminar stresses along interfaces *(n -1* equations)

$$\bar{\tau}^{k-1}\left(\bar{z}=h_{k-1}\right) = \bar{\tau}^k\left(\bar{z}=0\right) \tag{10b}$$

3. assuming the interlaminar stresses from the constitutive equations to be an average interlaminar stresses within a layer (*n* equations)

$$\int_0^{h_k}\bar{\tau}^k\left(\bar{z}\right)d\bar{z} = \frac{\bar{\tau}_b^k + \bar{\tau}_t^k}{2}h_k \tag{10c}$$

4. computing the jump in interlaminar stresses at each interface utilizing the 3D equations of equilibrium in terms of stresses (*n-1* equations)

$$\frac{\partial \bar{\tau}^{k-1}\left(\bar{z}=h_{k-1}\right)}{\partial \bar{z}}-\frac{\partial \bar{\tau}^{k}\left(\bar{z}=0\right)}{\partial \bar{z}}=\frac{\partial \bar{\tau}_{3D}^{k-1}}{\partial z}-\frac{\partial \bar{\tau}_{3D}^{k}}{\partial z} \tag{10d}$$

In (10d), $\bar{\boldsymbol{\tau}}_{3D}=\left\{\tau_{xz}^{3D} \quad \tau_{yz}^{3D} \quad \sigma_{zz}^{3D}\right\}^{T}$ is the vector of interlaminar stresses obtained from 3D equilibrium equations:

$$\tau_{xz,z}^{3D}=-\left(\sigma_{xx,x}^{3D}+\tau_{xy,y}^{3D}\right), \qquad \tau_{yz,z}^{3D}=-\left(\tau_{xy,x}^{3D}+\sigma_{yy,y}^{3D}\right), \qquad \sigma_{zz,z}^{3D}=-\left(\tau_{xz,x}^{3D}+\tau_{yz,y}^{3D}\right) \tag{11}$$

5. Numerical Examples

To validate the model and illustrate its capability for an accurate prediction of 3-D stress state in the laminated composite plate, illustrative numerical example is provided. The analyzed problem deals with the bending analysis of square simply supported laminated composite plate. The plate consists of 3 orthotropic material layers in cross-ply symmetric stacking sequence (0/90/0) and it is loaded by transverse distribution of constant pressure at the top surface of the plate, $q_t(x,y)=q_t$. Each layer is a unidirectional reinforced composite made of material with the following properties: $E_1/E_2 = 25$, $G_{12}/E_2 = G_{13}/E_3 = 0.5$, $G_{23}/E_2 = 0.2$, $\nu_{12} = \nu_{13} = \nu_{23} = 0.25$. Two different a/h ratios have been considered ($a/h = 4$ and $a/h = 10$), where h is the overall plate thickness and a is the side length of the plate. For the through-the-thickness interpolation, two models have been considered: (i) 3-layers (0/90/0) plate with $h_k=h/3$, and (ii) 6-layers (0/0/90/90/0/0) plate with $h_k=h/6$ (sublaminate concept).

Boundary conditions are prescribed edge nodes: $U^I= W^I=0$ for edge parallel to x-axis and $V^I= W^I=0$ for edge parallel to y-axis. To account for different plate dimensions, dimensionless displacement and stresses have been considered:

$$\bar{U}=\frac{100E_2h^2}{q_ta^3}u, \quad \left(\bar{\sigma}_x,\bar{\sigma}_y,\bar{\tau}_{xy}\right)=\frac{1}{q_t}\left(\frac{h}{a}\right)^2\left(\sigma_x,\sigma_y,\tau_{xy}\right), \quad \left(\bar{\tau}_{xz},\bar{\tau}_{yz},\bar{\sigma}_z\right)=\frac{1}{q_t}\frac{h}{a}\left(\tau_{xz},\tau_{yz},\sigma_z\right) \tag{12}$$

The convergence study of the present model is performed using both Q4 and Q8 elements with reduced integration, for three different mesh sizes: 4×4, 8×8 and 12×12. An additional comparison is made against the results obtained by Carrera & Ciuffreda [15], using LD3 theory (layerwise classical theory with cubic expansion through the thickness). The results are elaborated in Tables 1-4.

a/h=4, 3 layers	16Q8	64Q8	144Q8	16Q4	64Q4	144Q4	LD3 [15]
w (a/2, b/2, 0)	2.9499	2.9451	2.9452	3.2192	3.0037	2.9691	3.0446
σ_x (a/2, b/2, h/2)	1.0890	1.0233	1.0131	1.0269	1.0085	1.0080	1.1156
τ_{xy} (a, 0, h/2)	0.1008	0.0984	0.0972	0.0786	0.0873	0.0904	0.0973
τ_{xz} (0, b/2, 0)	0.4560	0.4352	0.4307	0.4120	0.4039	0.4002	0.4434

Table 1. Comparison of different mesh densities and element types to evaluate transverse displacement $\bar{U}$ and stresses $\bar{\sigma}_x, \bar{\tau}_{xy}$ and $\bar{\tau}_{xz}$ for 3-layers (0/90/0) thick laminated composite plate (a/h = 4)

a/h=4, 6 layers	16Q8	64Q8	144Q8	16Q4	64Q4	144Q4	LD3 [15]
w (a/2, b/2, 0)	3.0018	2.9996	2.9997	3.2795	3.0563	3.0237	3.0446
σ_x (a/2, b/2, h/2)	1.1786	1.1059	1.0949	1.1119	1.0867	1.0875	1.1156
τ_{xy} (a, 0, h/2)	0.1097	0.1115	0.1124	0.0868	0.0971	0.1017	0.0973
τ_{xz} (0, b/2, 0)	0.4613	0.4448	0.4422	0.4005	0.4035	0.4061	0.4434

Table 2. Comparison of different mesh densities and element types to evaluate transverse displacement $\bar{U}$ and stresses $\bar{\sigma}_x, \bar{\tau}_{xy}$ and $\bar{\tau}_{xz}$ for 6-layers (0/0/90/90/0/0) thick laminated composite plate (a/h = 4)

a/h=10, 3 layers	16Q8	64Q8	144Q8	16Q4	64Q4	144Q4	LD3 [15]
w (a/2, b/2, 0)	1.1308	1.1309	1.1309	1.2105	1.1480	1.1382	1.1541
σ_x (a/2, b/2, h/2)	0.9206	0.8638	0.8544	0.8602	0.8477	0.8473	0.8702
τ_{xy} (a, 0, h/2)	0.0605	0.0595	0.0589	0.0468	0.0528	0.0548	0.0597
τ_{xz} (0, b/2, 0)	0.6678	0.6366	0.6299	0.6170	0.6164	0.6182	0.6278

Table 3. Comparison of different mesh densities and element types to evaluate transverse displacement $\bar{U}$ and stresses $\bar{\sigma}_x, \bar{\tau}_{xy}$ and $\bar{\tau}_{xz}$ for 6-layers (0/0/90/90/0/0) thick laminated composite plate (a/h = 10)

a/h=10, 6 layers	16Q8	64Q8	144Q8	16Q4	64Q4	144Q4	LD3 [15]
w (a/2, b/2, 0)	1.1480	1.1480	1.1480	1.2295	1.1655	1.1554	1.1541
σ_x (a/2, b/2, h/2)	0.9397	0.8819	0.8723	0.8818	0.8656	0.8645	0.8702
τ_{xy} (a, 0, h/2)	0.0620	0.0614	0.0612	0.0481	0.0546	0.0567	0.0597
τ_{xz} (0, b/2, 0)	0.6678	0.6381	0.6321	0.6678	0.6030	0.6104	0.6278

Table 4. Comparison of different mesh densities and element types to evaluate transverse displacement $\bar{U}$ and stresses $\bar{\sigma}_x, \bar{\tau}_{xy}$ and $\bar{\tau}_{xz}$ for 6-layers (0/0/90/90/0/0) thick laminated composite plate (a/h=10)

The results presented in Tables 1-4 indicate that the proposed model is capable to accurately predict the stress-deformation state of the cross-ply laminated composite plate. After omitting the results for coarse meshes (16Q4 and 16Q8) which showed to be inaccurate, the average relative differences Δ = (result – reference) / reference [%] are calculated and given in Table 5:

Δ [%]	a/h = 4		a/h = 10	
	3 layers	6 layers	3 layers	6 layers
w	2.6	1.0	1.5	0.5
σ_x	9.2	2.0	1.9	0.7
τ_{xy}	4.7	8.7	5.4	4.7
τ_{xz}	5.8	4.5	1.3	2.3

Table 5. Average relative differences of considered models against [15] for different side-to-thickness ratios and different interpolation through the thickness

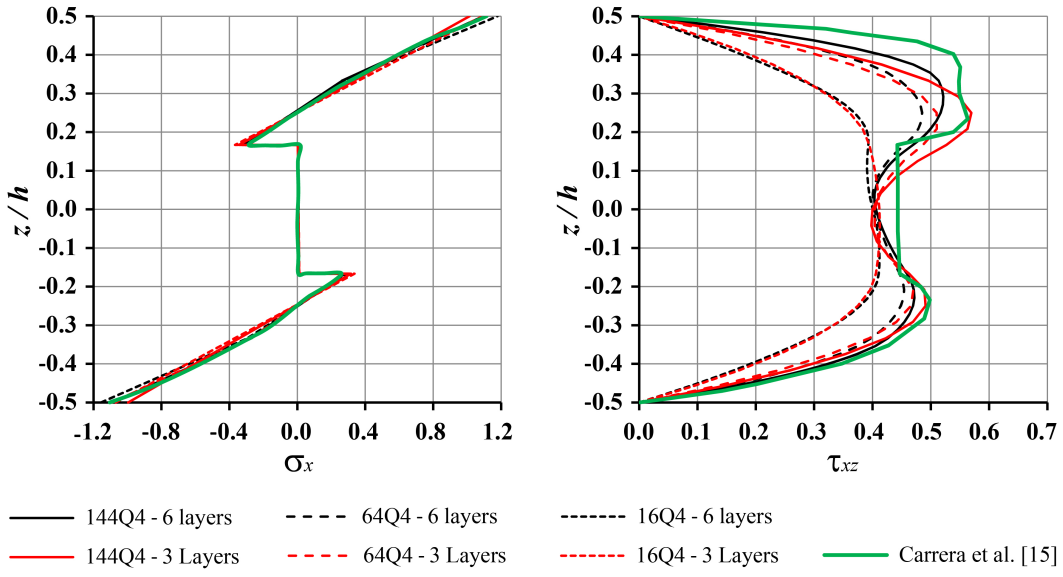

Fig. 2. Comparison of different mesh densities of FLWT-Q4 elements to evaluate through-the-thickness distribution of stresses $\bar{\sigma}_x$ and $\bar{\tau}_{xz}$ for thick laminated composite plate (a/h = 4)

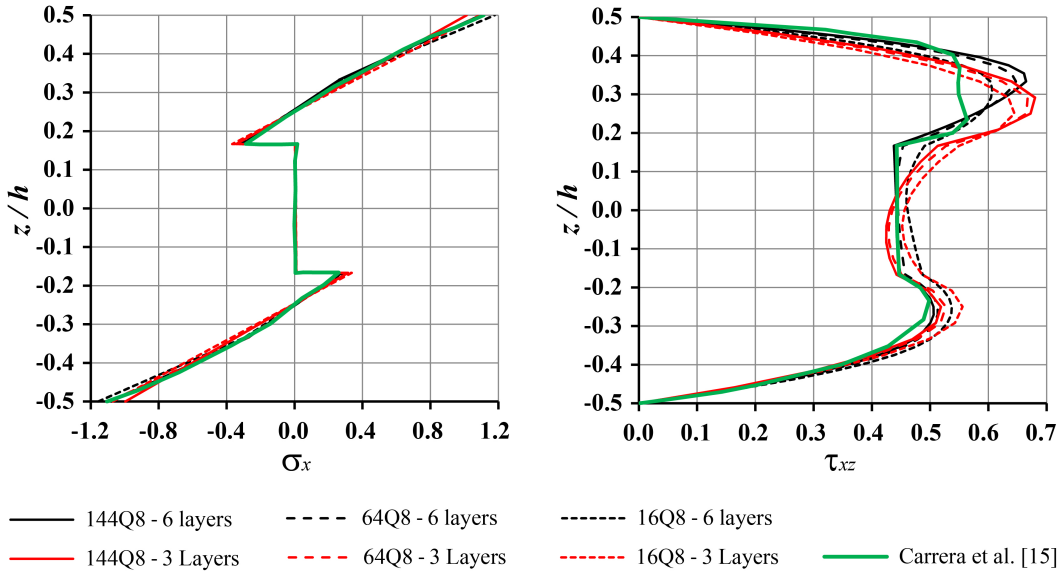

Fig. 3. Comparison of different mesh densities of FLWT-Q8 elements to evaluate through-the-thickness distribution of stresses $\bar{\sigma}_x$ and $\bar{\tau}_{xz}$ for thick laminated composite plate (a/h = 4)

Obviously, z-refinement plays very important role in the accuracy of the proposed models, where 6-layers model showed the advantage over the 3-layers one. The highest discrepancies are obtained for shear stresses τ_{xy} and τ_{xz}, where cubic expansion of the displacement components used in the LD3 theory [15] showed the advantage over the linear layerwise expansion in FLWT.

The agreement is better for a/h = 10 (the average difference of all quantities is 2.3%) in comparison with a/h = 4 (the average difference of all quantities is 4.8%). Finally, for the calculation of interlaminar stress τ_{xz}, the Q8 model is recommended which showed only marginal differences in comparison with [15] (for all quantities, Δ=1.3% for a/h=4, Δ=1.0% for a/h = 10).

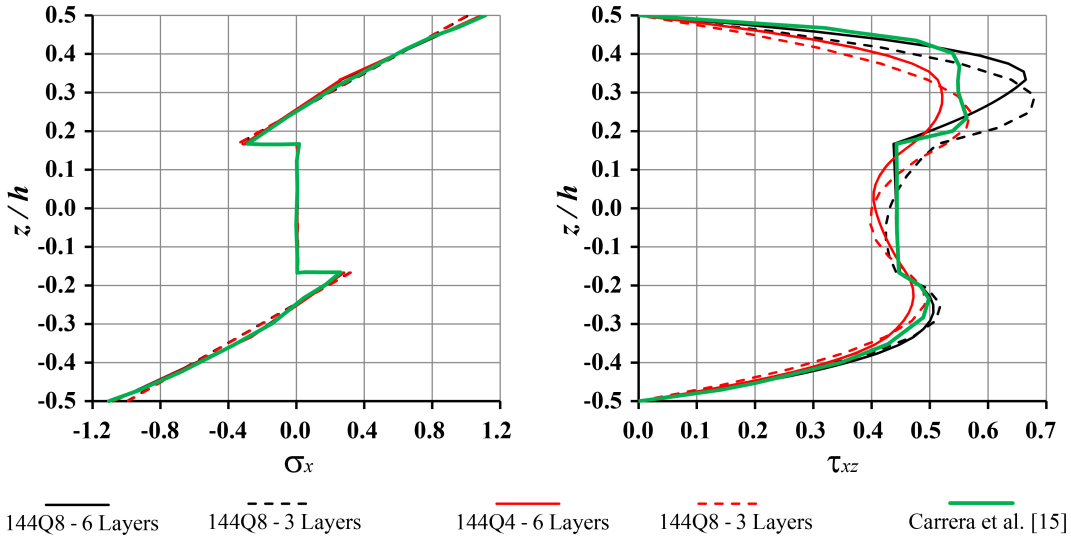

Fig. 4. Comparison of different element types and through-the-thickness interpolations to evaluate distribution of stresses $\bar{\sigma}_x$ and $\bar{\tau}_{xz}$ vs. z-coordinate, for thick laminated composite plate (a/h = 4)

Through-the-thickness distribution of stresses $\bar{\sigma}_x$ and $\bar{\tau}_{xz}$ for thick laminated composite plate (a/h = 4) is plotted in Figs. 2-4, for different mesh densities, z-refinements and different

element types. The results are compared against the results from [15] using LM3 theory (mixed layerwise theory with cubic expansion). All models showed the possibility for accurate determination of σ_x. However, the results for shear stress τ_{xz} distribution showed the advantage of Q8 over Q4 elements.

To illustrate the capability of the object-oriented software framework to visualize the stress distribution, GiD visualization of stresses obtained using 64Q8 and 64Q4 elements is plotted in Figs. 5-6 against the results of the commercial software Abaqus (64 C3D20R finite elements). Excellent agreement is obtained, although a considerably lower number of degrees of freedom is employed in the FLWT-based models in comparison with 3-D (solid) models in Abaqus.

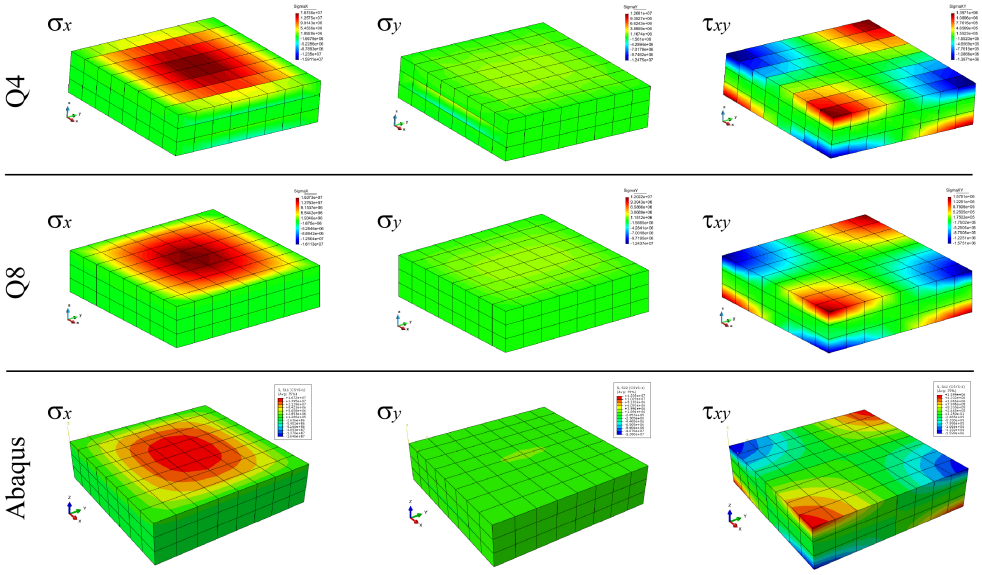

Fig. 5. Distribution of σ_x, σ_y and τ_{xy} in simple supported laminated composite plate (a=1.2m, h=0.3m, E_1=25GPa, E_2=1GPa, G_{12}=G_{13}=0.5GPa, G_{23}=0.2GPa, q_t=1MPa) obtained using 64 FLWT-Q4, 64 FLWT-Q8 and 64 C3D20R elements (Abaqus)

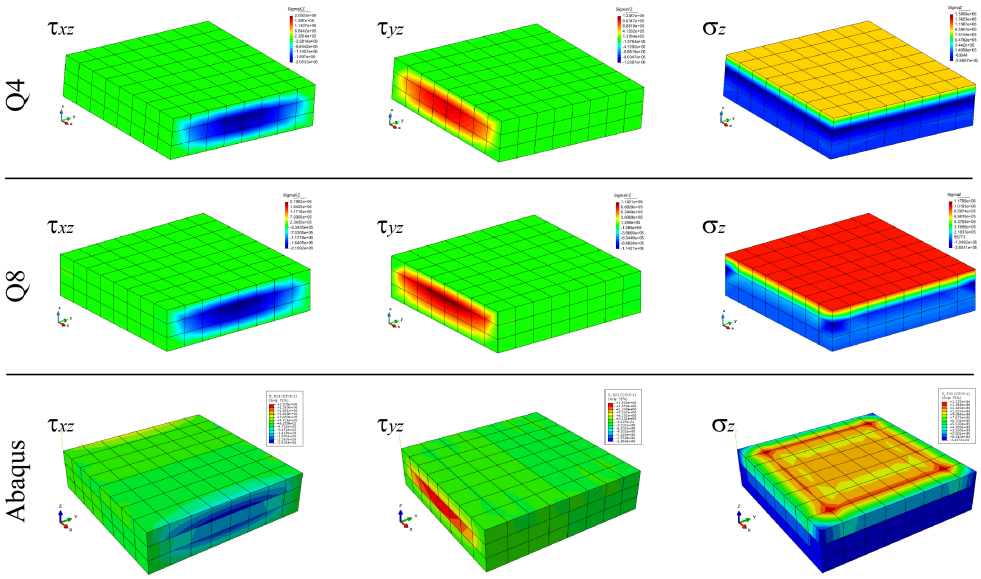

Fig. 6. Distribution of interlaminar stresses τ_{xz}, τ_{yz} and σ_z in laminated composite plate (a=1.2m, h=0.3m, E_1=25GPa, E_2=1GPa, G_{12}=G_{13}=0.5GPa, G_{23}=0.2GPa, q_t=1MPa) obtained using 64 FLWT-Q4, 64 FLWT-Q8 or 64 C3D20R elements (Abaqus)

6. Conclusions

In the paper, a family of layered quadrilateral finite elements based on the full layerwise theory of Reddy (FLWT) has been developed and implemented in the object-oriented MATLAB code in conjunction with original GiD interface for pre- and post-processing. Original procedure for post-processing of stresses is presented. The presented approach is validated against the 3-D (solid) models of LCPs in ABAQUS, as well as using the available data from the literature, confirming the high reliability of the presented procedure.

Future work includes the implementation of triangular FLWT-T3 and FLWT-T6 elements in the presented framework. The first-ply failure analysis will be conducted using the above method.

Acknowledgments

The financial support of the Ministry of Education, Science and Technological Development, Serbia, through the projects TR-36046 and TR-36048, is acknowledged. The full license of GiD software is provided by the Institute for Structural Mechanics, Ruhr University Bochum.

References

[1] Kirchhoff, G., *Uber das Gleichgwich und die Bewegung einer Elastischen Scheibe*, Journal fur Angewandte Mathematik, Vol. 40, 51-88, 1850.
[2] Mindlin, R. D., *Influence of rotatory inertia and shear on flexural motions of isotropic, elastic plates*, Journal of Applied Mechanics, Vol. 18, No. 1, 31-38, 1951.
[3] Reddy, J. N., *A simple higher-order theory for laminated composite plates*, Journal of Applied Mechanics, Vol. 51, 745-752, 1984.
[4] Carrera, E., *Theories and finite elements for multilayered, anisotropic, composite plates and shells*, Archives of Computational Methods in Engineering, Vol. 9, No. 2, 87-140, 2002.
[5] Lur'e, N., Shumova, P., *Kinematic models of refined theories concerning composite beams, plates, and shells*, Mechanics of Composite Materials, Vol. 32, No. 5, 422-430, 1996.
[6] Reddy, J. N., Robbins, D. H., *Theories and computational models for composite laminates*, Applied Mechanics Reviews, Vol. 47, 147-165, 1994.
[7] Marjanović, M., Vuksanović, Dj., *Layerwise solution of free vibrations and buckling of laminated composite and sandwich plates with embedded delaminations*, Composite Structures, Vol. 108, 9–20, 2014.
[8] Marjanović, M., Vuksanović, Dj., Meschke, G., *Geometrically nonlinear transient analysis of delaminated composite and sandwich plates using a layerwise displacement model with contact conditions*, Composite Structures, Vol. 122, 67–81, 2015.
[9] Marjanović, M., Meschke, G., Vuksanović, Dj., *A finite element model for propagating delamination in laminated composite plates based on the Virtual Crack Closure method*, Composite Structures, Vol. 150, 8-19, 2016.
[10] Ćetković, M., Vuksanović, Dj., *Bending, free vibrations and buckling of laminated composite and sandwich plates using a layerwise displacement model*, Composite Structures, Vol. 88, No. 2, 219-227, 2009.
[11] Reddy, J. N., *Mechanics of laminated composite plates and shells: theory and analysis*, CRC Press, Boca Raton, Florida, 2004.
[12] MATLAB R2011b, The MathWorks, Inc., Natick, Massachusetts, USA.
[13] GiD Customization Manual. CIMNE – International Center for Numerical Methods in Engineering, 2016.
[14] ABAQUS User Manual 6.9. DS SIMULIA Corp., Providence, Rhode Island, USA, 2009.
[15] Carrera, E., Ciuffreda, A., *A unified formulation to assess theories of multilayered plates for various bending problems*, Composite Structures, Vol. 69, No. 3, 271-293, 2005.